Published in final edited form as:
Mol Cancer Ther. 2014 January ; 13(1): 122–133. doi:10.1158/1535-7163.MCT-12-1232.

Response to MLN8237 in pancreatic cancer is not dependent on RalA phosphorylation

Nicole F. Neel[1], **Jeran K. Stratford**[2], **Vaishali Shinde**[4], **Jeffrey A. Ecsedy**[4], **Timothy D. Martin**[1,2], **Channing J. Der**[1,2], and **Jen Jen Yeh**[1,2,3]

[1]Lineberger Comprehensive Cancer Center, University of North Carolina at Chapel Hill, Chapel Hill, NC 27599

[2]Department of Pharmacology, University of North Carolina at Chapel Hill, Chapel Hill, NC 27599

[3]Department of Surgery, University of North Carolina at Chapel Hill, Chapel Hill, NC 27599

[4]Millennium: The Takeda Oncology Company

Abstract

The high prevalence of *KRAS* mutations and importance of the RalGEF-Ral pathway downstream of activated K-Ras in pancreatic ductal adenocarcinoma (PDAC) emphasize the importance of identifying novel methods by which to therapeutically target these pathways. It was recently demonstrated that phosphorylation of RalA S194 by Aurora A kinase is critical for PDAC tumorigenesis. We sought to evaluate the Aurora A kinase-selective inhibitor MLN8237 as a potential indirect anti-RalA targeted therapy for PDAC. We utilized a site-specific phospho-S194 RalA antibody and determined that RalA S194 phosphorylation levels were elevated in a subset of PDAC cell lines and human tumors relative to unmatched normal controls. Effects of MLN8237 on anchorage-independent growth in PDAC cell lines and growth of patient-derived xenografts (PDX) were variable, with a subset of cell lines and PDX showing sensitivity. Surprisingly, RalA S194 phosphorylation levels in PDAC cell lines or PDX tumors did not correlate with MLN8237 responsiveness. However, we identified Ki67 as a possible early predictive biomarker for response to MLN8237 in PDAC. These results indicate that MLN8237 treatment may be effective for a subset of PDAC patients independent of RalA S194 phosphorylation. Ki67 may be an effective pharmacodynamic biomarker to identify response early in the course of treatment.

Keywords

Aurora A kinas; RalA; pancreatic cancer; MLN8237; biomarker

INTRODUCTION

Pancreatic ducal adenocarcinoma (PDAC) is the fourth leading cause of death in the United States accounting for approximately 37,000 deaths annually with a five year survival rate of less than five percent (1). Gemcitabine remains the most effective treatment for patients with locally advanced and metastatic PDAC, with only a 24% response rate and median survival

Corresponding author: Jen Jen Yeh, M.D., CB# 7213, 1150 Physicians Office Building, 101 Manning Drive, Chapel Hill, NC 27599-7213, Tel: (919) 966-5221, Fax: (919) 966-6673, jjyeh@med.unc.edu.

Conflicts of interest:

1. Vaishali Shinde and Jeffrey A. Ecsedy are employees of Millenium: The Takeda Oncology Company
2. Nicole F. Neel, Timothy D. Martin, Channing J. Der,and Jen Jen Yeh have no conflicts of interest.

of only 5.6 months. Therefore, there remains a crucial need for the development and evaluation of new targeted therapies (2, 3).

The frequent mutational activation of *KRAS* in PDAC and critical importance of K-Ras-driven signaling in PDAC progression has led to increased efforts to identify K-Ras-targeted therapies. There is increasing evidence for the importance of the RalA and RalB small GTPases in mutant Ras-driven oncogenesis (4, 5). RNAi knockdown of endogenous RalA in PDAC cells significantly impaired anchorage-independent growth whereas knockdown of RalB impaired Matrigel invasion in vitro and experimental metastasis in vivo (6). Importantly, RalA-GTP and RalB-GTP levels were significantly higher in PDAC cell lines and in patient tumors relative to normal matched and unmatched samples (6, 7). Taken together, these studies suggest that therapeutic inhibition of Ral may be an effective therapy for *KRAS* mutant PDAC.

Like Ras, Ral is a GTPase and therefore not a tractable target for direct inhibition. However, we and others have determined that Ral growth regulatory activities are regulated by phosphorylation. Hahn and colleagues showed that serine-threonine protein phosphatase 2A dephosphorylation of RalA at S183 and S194 abolished RalA transforming activity (8). Two other studies determined that S194 could be phosphorylated by Aurora A and that this phosphorylation was essential for RalA transforming activity (9) and RalA-dependent PDAC anchorage-independent and tumorigenic growth (10). Aurora A phosphorylation alters RalA subcellular localization and interaction with effectors (10, 11). Activation of Aurora A promotes mitochondrial localization of RalA and promotes mitochondrial fission (11), which may present a mechanism for Aurora A contribution to tumorigenesis (12). These findings suggest that protein kinas inhibitors may be an effective approach for inhibition of Ral.

Aurora A kinas (AAK) is a member of a family of serine-threonine kinases that regulate mitosis. A number of proteins associated with mitosis are phosphorylated by AAK through spatially and temporally controlled mechanisms (13). Amplification of the *AURKA* gene is commonly found in a number of malignancies (14–16) and overexpression of AAK is associated with high tumor grade and poor prognosis (15, 17–20). Surprisingly, it does not independently possess transforming activity in rodent cells or mouse models of PDAC (21, 22), suggesting the necessity to cooperate with other oncogenic pathways to promote tumorigenesis.

This evidence suggests that targeting RalA phosphorylation with AAK inhibitors may be a viable therapeutic option for the treatment of pancreatic cancer. MLN8237 is a novel and selective AAK inhibitor that has entered Phase III clinical trials. We investigated the effectiveness of MLN8237 at inhibiting anchorage-independent growth of PDAC cell lines and patient-derived xenograft (PDX) growth in vivo. PDX models maintain heterogeneity and allow tumor cell growth in the context of a microenvironment (23). This is especially relevant in PDAC due to the contribution of desmoplasia to the pathology and treatment of the disease (24, 25). The method is previously described (26–29) and involves implantation of small tumor fragments taken from the patient and directly implanted into immunodeficient mice. Tumors are subsequently propagated and expanded into several animals and subjected to treatment with anticancer therapies.

In the current study, we found that S194 RalA phosphorylation was increased in a subset of PDAC cell lines and human tumors and correlated with autophosphorylation of Aurora A (indicative of activation). This suggested that targeting RalA phosphorylation with AAK inhibitors may prove to be a viable therapeutic option for the treatment of pancreatic cancer.

Therefore the goal of the current study was to investigate whether an AAK selective inhibitor, MLN8237, may be used as a therapeutic strategy to target RalA in PDAC.

MATERIALS AND METHODS

Human pancreatic tumor cell lines

The BxPC3, MIA PaCa-2, HPAC, Panc 02.03, AsPC-1, SW1990, HPAF-II, CFPAC-1, PANC-1, Capan-1, Capan-2, Panc 10.05, and T3M4 PDAC cell lines were obtained from ATCC (Manassas, VA). Cell lines were passaged for fewer than six months upon acquisition from ATCC. ATCC authentication was performed using short tandem repeat DNA profiling. HuPT3 cells were obtained from Dan Billadeau (Mayo Clinic, Rochester, MN). No authentication was performed on the HuPT3 cell line by the authors. The immortalized human pancreatic duct-derived (HPNE) cells were described previously (30, 31).

Western blot analysis

Whole cell lysates were isolated in NP40 lysis buffer. Human tumor lysates from flash frozen samples were homogenized in NP40 lysis buffer, resolved by SDS-PAGE, and evaluated by western blot analyses with the primary antibodies: rabbit anti-phospho-RalA (S194) (Millipore), mouse anti-RalA (BD Bioscience), rabbit anti-phospho-Aurora A (T288) (Cell Signaling Technology), rabbit anti-Aurora A (Millipore), mouse anti-vinculin (Sigma), mouse anti-β-tubulin (Sigma), mouse anti-HA (Covance) and species appropriate HRP-conjugated secondary antibodies (Pierce). Membranes were subjected to detection using ECL. Densitometry measurements were performed using ImageJ software.

Purification of recombinant GST-RalA and in vitro phosphorylation with PKA

RalA cDNA was subcloned into pGEX-2T in frame with sequences encoding an N-terminal glutathione S-transferase (GST) tag using the BamHI site. pGEX-2T RalA, and empty vector were transformed into Rosetta 2 bacterial expression cells. Protein expression was induced with 1 mM IPTG. Bacterial pellets were resuspended in Triton-X-100 based lysis buffer and sonicated. GST-bound proteins were isolated with glutathione-sepharose beads. Five μg of purified GST or GST-RalA was incubated with 2500 U cAMP-dependent protein kinas A (PKA) catalytic subunit (New England Biolabs) with or without 100 mM ATP for 30 min at 30°C. Reactions were separated by SDS-PAGE, transferred to polyvinylidene fluoride (PVDF) membrane, and stained with 0.1% amido black staining solution. Membranes were destained, imaged, and subjected to western blot analysis.

Synchronization of PDAC cell lines

To clearly visualize pT288 Aurora A protein levels, cells were synchronized prior to lysis. Cells were treated with either dimethysulfoxide (DMSO; vehicle) or indicated concentrations of MLN8237. Prior to harvesting and during the drug treatment cells were synchronized by treating with 2 mM thymidine for 18 h. Thymidine was removed and cells were released for 8 h prior to treating with 100 ng/ml nocodazole for 16 h in order to block cells in mitosis.

Anchorage-independent growth assay

$2–4 \times 10^3$ cells were seeded in a 12-well culture dish as described previously (32, 33). DMSO or MLN8237 were included in the agar and in growth medium throughout the assay. All conditions were seeded in triplicate. After 2–6 weeks of growth, colonies were stained with 5 mg/ml 1-(4,5-Dimethylthiazol-2-yl)-3,5-diphenylformazan (MTT) (Sigma) and those of >30 cells in size were scored.

Anchorage-dependent growth assay with MTT

$1–3 \times 10^3$ cells were seeded in a 96-well plate and cells were allowed to attach overnight. DMSO or MLN8237 was added to the cells the following day and incubated for 48 h. MTT was incubated in each well for 4 h at 37°C. The cells were lysed with DMSO and absorbance was read at 550/490nm.

Calculation of IC50 values

IC50 values were calculated for the anchorage-dependent assays by normalizing the absorbance in the MLN8237-treated wells to that in the DMSO wells. IC50 values were calculated for the soft agar assays by normalizing the number of colonies in the MLN8237-treated cells to the number of colonies in the DMSO control. The fraction of cells affected was calculated and entered into the CalcuSyn program (Biosoft). Dose effect curves and IC50 values were calculated.

Plasmids and retroviral infection

pSUPER.retro.blast retrovirus plasmids encoding shRNA directed against green fluorescent protein (GFP; non-specific control) (34) and RalA have been validated and characterized previously (35). pBabe.puro expression vectors encoding *H. sapiens* RalA cDNA have been described previously (35). Site-directed mutagenesis was performed to generate phosphorylation mutants followed by verification by sequencing. The pBabe.hygro.HA.Aurora A T288D expression plasmid was obtained from Christopher Counter (Duke University, Durham, NC).

Animal studies

Studies were performed in accordance with protocols approved by the University of North Carolina Institutional Animal Care and Use Committee. The PDAC PDX model was established as previously described (27). Briefly, de-identified tumors released by the Tissue Procurement Core Facility under an IRB-approved protocol were mixed with Matrigel and grafted into athymic (nu/nu) or NOD SCID gamma (NSG) mice. Tumors were allowed to grow to maximal dimension, passaged and expanded. Tumor histology was confirmed by hematoxylin and eosin staining prior to expansion. Nine PDX tumors were expanded in athymic (nu/nu) mice and treatment began when the tumors reached a median volume of 97.5 mm^3 (range 55–140). Tumor volume was calculated with the following formula: $(length/2)*width^2$. A 7.81 mg/ml MLN8237 sodium salt solution was prepared fresh before each study in vehicle (10% 2-hydroxylpropyl-β-cyclodextrin/1% sodium bicarbonate in sterile water). Animals were dosed via oral gavage daily with either vehicle, 10, or 30 mg/kg (maximum tolerated dose (MTD)) MLN8237 for 28 days or until either dimension of the tumor reached 2 cm. Tumor volume was monitored by caliper measurements. Each vehicle and treatment group consisted of 4–6 animals. The animals were sacrificed on Day 28, 2 h after the final dose was administered. Tumors were harvested and halved. One portion was flash frozen and stored at −80°C and the other was fixed for 24 h in 10% formalin and transferred to 70% ethanol for storage. For single dose studies, mice bearing tumors (median volume 75 mm^3) (3–4 animals per time point) were treated with 30 mg/kg MLN8237 and sacrificed at the indicated times following treatment. Tumors were harvested and processed as above. Tumor growth inhibition (TGI) was defined as >30% growth inhibition compared to vehicle. Regression was defined as any decrease in tumor size from the treatment initiation.

Ki67 staining of xenograft tumor tissue

Four micron sections were prepared from paraffin-embedded tumors and dewaxed in xylene followed by graded alcohol series to water. Steam heat induced epitope recovery (SHIER)

was used for the rabbit polyclonal Ki67 antibody (Vector Labs) with SHIER1 solution for 20min in the capillary gap in the upper chamber of a Black and Decker Steamer. The immunohistochemistry procedure was automated using TechMate 500 or 1000 (Roche Diagnostics). After staining, slides were dehydrated through an alcohol series to absolute ethanol followed by xylene rinses. Slides were permanently coverslipped with glass coverslips and CytoSeal (Thomas Scientific). Positive staining was indicated by the presence of a brown chromogen (DAB-HRP) reaction product. Hematoxylin counterstain was used to assess cell and tissue morphology. For quantitative analysis whole PDX tumors were scanned at 20X with Olympus BX61VS equipped with a VS110 SH5 robotic stage. A 4 mm^2 area chosen as representative of overall positive cell frequency was cropped and saved as a JPEG 2000 image file. Images were analyzed using ImagePro 6.1 (Media Cybernetics Inc.) to count the total number of pHH3 and Ki67 positive cells. Color thresholds, area filters, and splitting tools were used to obtain a realistic segmentation of the tumor cells. The positive percentage of Ki67 cells was obtained for each sample by dividing the total number of Ki67 positive cells by the total number of hematoxylin stained cells.

RalA Immunofluorescence and Confocal Microscopy

Cells were seeded on coverslips, incubated overnight, treated with either vehicle of 100nM MLN8237 for 48 h, fixed in 4% paraformaldehyde in PBS, permeabilized in 0.5% Triton X-100/PBS, and blocked in 3% bovine serum albumin/PBS. Coverslips were then incubated with mouse anti-RalA antibody (BD Biosciences) and fluorescent phalloidin. Confocal images were acquired using a LSM-710 Meta laser scanning microscope (Carl Zeiss) with a 63X 1.3 numerical aperture oil immersion lens and images were processed by Photoshop software (Adobe Systems).

RESULTS

Effects on anchorage-dependent and -independent growth of PDAC cell lines are variable in response to MLN8237

We investigated whether MLN8237 was effective at inhibiting anchorage-dependent and -independent growth of PDAC cell lines. AAK activity was assessed by the level of auto-phosphorylation at threonine 288 (pT288 Aurora A), required for AAK activity, in PDAC cell lines synchronized with a thymidine/nocodazole block (Fig. 1A). We evaluated the effects of MLN8237 on anchorage-dependent and -independent growth in a panel of ten PDAC cell lines with variable T288 Aurora A phosphorylation levels. Although the cell lines exhibited a range of sensitivity in anchorage-dependent MTT assays, IC50 values from 293nM to greater than 10,000 nM, MLN8237 effects on anchorage-independent growth were much more potent. Brdu assays were also used to assess the effects of MLN8237 on anchorage-dependent growth in Capan-2 and MIA PaCa-2 cell lines. The IC50 values were 1372.8nM and 147.8nM in Capan-2 and MIA PaCa-2 cell lines, respectively. The cell lines exhibited variable sensitivity to MLN8237 in soft agar with IC50 values ranging from 3.3 to 236.8nM (Table 1 and Fig. 1B, C). Following treatment with MLN8237 we observed a concentration-dependent decrease in Aurora A T288 phosphorylation (Fig. 1D), validating that MLN8237 was effective at inhibiting AAK activity.

MLN8237 inhibits tumor growth in a subset of PDAC PDX tumors

Because the PDX model has emerged as a better predictive model for evaluation of novel therapeutics (23, 27), we assessed the ability of MLN8237 to inhibit tumor growth in this model. The passaged tumors maintained the original tumor architecture observed in the initial patient tumor (Fig. 2A), indicating that the tumor morphology remains consistent throughout passage in the animals. Mice with early passage PDX were treated with vehicle, 10 mg/kg or 30 mg/kg MLN8237 for 28 days once tumor size reached a median size of 97.5

mm^3. Tumors were harvested for biomarker analysis on day 28 of treatment. We found that four of the seven xenografts analyzed exhibited either regression or tumor growth inhibition (TGI) at 30 mg/kg (Table 2 and Fig. 2B). We observed no significant responses at 10 mg/kg (Supplementary Fig. 1B)

RalA is phosphorylated on serine 194 in a subset of human PDAC cell lines and patient tumor samples and correlates with pT288 Aurora levels

We next sought to identify a activity-activity specific biomarker for predicting MLN8237 responsiveness in PDAC cell lines and PDX tumors. We investigated whether RalA S194 phosphorylation was a biomarker for responsiveness. In order to determine the in vivo and clinical incidence of RalA S194 phosphorylation, we examined the phosphorylation levels using a rabbit polyclonal antibody made against a RalA peptide sequence that contained phosphorylated S194. We determined that this antibody was specific for RalA phosphorylated at S194 using lysates from PANC-1 cells expressing RalA-specific shRNA to suppress endogenous RalA expression and with ectopic expression of wild type or S194A RalA from RNAi-insensitive cDNA expression vectors (Fig. 3A). In order to further validate the antibody, we phosphorylated GST-RalA in vitro using the purified catalytic subunit of PKA (previously shown to phosphorylate RalA in vitro (36)) and found that the antibody specifically recognized purified GST-RalA in the presence of PKA and ATP (Supplementary Fig. 2).

RalA S194 phosphorylation levels were examined in patient samples and high levels were observed in a subset of the tumors compared to unmatched normal controls (Fig. 3C). Lysates from a panel of PDAC cell lines were examined for S194 phosphorylation levels and a subset of PDAC cell lines showed high levels of phosphorylation compared to non-transformed human nestin-positive pancreatic epithelial cells (HPNE) (Fig. 3B). Interestingly, all cell lines with high levels of pS194 RalA (BxPC3, MIAPaCa-2, Capan-2, Panc 10-05, SW1990, and HuPT3) also had high levels of pT288 Aurora A (Fig. 1A and Fig. 3B). However, there was not a direct correlation between MLN8237 sensitivity and the level of basal RalA S194 phosphorylation. The correlation coefficient between pS194 RalA levels and soft agar IC50 values was −0.41 but this was not significantly different from zero (p-value 0.23). We observed no significant reduction in S194 RalA phosphorylation following MLN8237 treatment. Furthermore, the trends in the changes in pS194 RalA phosphorylations levels following treatment did not vary with MLN8237 sensitivity.

Finally, vehicle treated PDX tumors were examined to determine whether basal RalA S194 phosphorylation levels were predictive of responsiveness. We found no correlation between RalA S194 phosphorylation levels and tumor response to MLN8237, suggesting that RalA phosphorylation was not a predictive biomarker (Fig. 3D–E). RalA phosphorylation levels were also examined following treatment with MLN8237 to determine whether changes in phosphorylation occurred with treatment. We observed no consistent changes in RalA S194 phosphorylation following MLN8237 treatment (Supplementary Fig. 3) in responders (PancT4) versus non-responders (PancT6). RalA phosphorylation was also examined in tumors from mice subjected to short-term (4, 8, and 24 h) MLN8237 treatments and no consistent changes were noted (data not shown).

MLN8237 treatment does not alter intracellular RalA localization in PDAC cell lines

RalA S194 phosphorylation by AAK can alter subcellular localization (10). We investigated whether MLN8237 treatment altered the intracellular localization of RalA in four PDAC cells lines; three with low (HuPT3, CFPAC-1, and Panc10.05) and one with high (HPAC) IC50 values in anchorage-independent growth assays. Intracellular RalA localization

remained unchanged following 48 h of treatment with 100nM MLN8237 in all four cell lines (Fig. 4A–D).

Expression of a RalA S194 phosphomimetic mutant in PDAC cells enhances anchorage-independent growth but does not diminish MLN8237 responsiveness

To further investigate RalA phosphorylation as a target of MLN8237 we expressed a S194 phosphomimetic mutant (S194D) as a putative Aurora A-independent variant in CFPAC-1 and MIA PaCa-2 cells (Fig. 5A) and evaluated anchorage-independent growth. As shown in Fig. 5B, ectopic expression of the S194D RalA mutant enhanced anchorage-independent growth two to three-fold when compared to empty vector controls. However, expression of this Aurora A-independent RalA variant did not reduce the sensitivity of PDAC cells to treatment with MLN8237 (Table 3 and Fig. 5B), suggesting that RalA may not be a dominant target of MLN8237 through inhibition of Aurora A. In addition, cells expressing S194D RalA exhibited decreases in Aurora A T288 phosphorylation similar to those seen in vector control cells (Fig. 5C).

Ki67 is a possible early biomarker for pancreatic PDX response to MLN8237

We sought to identify a biomarker that would indicate responsiveness in tumors treated with MLN8237. Increases in mitotic index, as quantitated by the phosphorylation levels of S10 in histone H3, were shown to be an early pharmacodynamic biomarker of response for Aurora A inhibition to the AAK inhibitor MLN8054 (37). Therefore, we investigated whether mitotic index could serve as a biomarker for MLN8237 responsiveness in our model. We examined the percentage of phosphorylated S10 histone H3-positive cells in responsive and non-responsive tumors treated with either vehicle or 30 mg/kg MLN8237 and harvested after 4 h, 8 h, 12 h, and 24 h. There was no significant increase in mitotic index in responsive or non-responsive tumors (Supplementary Fig. 4A). This was also true in the tumors treated for 28 days with vehicle or 30 mg/kg MLN8237 (Supplementary Fig. 4B), suggesting that mitotic index was not a biomarker for responsiveness in our PDX model.

The expression of Ki67 in the nucleus is restricted to proliferating cells. Ki67 staining of tumors is often used as a diagnostic and prognostic indicator for many tumor types, particularly in breast and prostate tumors (38). We examined the percentage of Ki67-positive nuclei in tumors that were responsive (PancT4) and non-responsive (PancT6) to MLN8237 treatment. The level of Ki67-positive nuclei was examined in PancT4 and PancT6 tumors treated with a single dose of MLN8237 (30 mg/kg) and harvested after 4 h, 8 h, and 12 h and in tumors dosed for 28 days with MLN8237 (30 mg/kg). There was a significant reduction in the Ki67-positive nuclei in the PancT4 tumors 4 h, 8 h, and 24 h after MLN8237 treatment (Fig. 6A, B). Although each individual harvest time point was not statistically significant due to limited sample size, the reduction in Ki67-positive nuclei at all time points combined was significant. There was no change in Ki67-positive nuclei following MLN8237 treatment in the PancT6 tumors at any of the time points (Fig. 6A, B). A similar trend was observed in the tumors treated for 28 days with MLN8237 (Fig. 6C). As seen with the single treatment time points, there was no change in the percentage of Ki67-positive nuclei in the PancT6 tumors following 28 days of MLN8237 treatment (Fig. 6C). These data suggest that Ki67 may be an early pharmacodynamic biomarker to identify tumor responsiveness after treatment with MLN8237.

DISCUSSION

The high prevalence of activating *KRAS* mutations in PDAC tumors and apparent *KRAS* oncogene addiction in pancreatic tumors (39) (40) emphasizes the importance of identifying anti-Ras therapies in the treatment of pancreatic cancer patients. Studies demonstrated the

importance of RalA and, more specifically, phosphorylation at S194 by AAK, in tumor development (6, 7, 10). The importance of RalA S194 phosphorylation in tumorigenesis makes AAK an attractive druggable target downstream of oncogenic Ras activation. The previous studies identifying RalA S194 phosphorylation relied primarily on ectopic expression of phosphorylation-deficient and phosphomimetic mutants and endogenous RalA-depleted PDAC cells. We therefore sought to evaluate endogenous RalA S194 phosphorylation levels in PDAC cell lines and human tumors using a S194 phospho-specific antibody. Our finding that RalA S194 phosphorylation levels were elevated in a subset of cell lines and tumors prompted us to hypothesize that anti-RalA targeted therapies may benefit those patients exhibiting elevated phosphorylation.

The recent characterization of RalA S194 as a substrate for AAK (9, 10) and our finding that RalA S194 phosphorylation levels correlated with Aurora A activation, as indicated by T288 phosphorylation, prompted us to investigate whether MLN8237 could be an effective anti-RalA therapy for pancreatic cancer. Most cell lines were largely insensitive to MLN8237 using the MTT assay to assess anchorage-dependent growth. However, studies from our laboratory and previous studies (41) have demonstrated much lower IC50 values using the BrdU assay, which suggests that the MTT assay is not a sensitive assay for MLN8237 activity. We found that a subset of cell lines showed inhibition of anchorage-independent growth after treatment of MLN8237 at nanomolar concentrations. However, we were unable to correlate this with RalA S194 phosphorylation levels. AAK activity is temporally controlled with peak activity during mitosis (42). It is possible that Aurora A phosphorylation of RalA at S194 is strictly temporally controlled, making it difficult to observe consistent changes following MLN8237 treatment in an asynchronous cell population. However, our data demonstrating that overexpression of a phosphomimetic (S194D) RalA mutant does not reduce sensitivity to MLN8237 inhibition of anchorage-independent growth argues that perhaps RalA phosphorylation is not a critical target for MLN8237 anti-tumor activity. We also found that RalA localization was unaffected by treatment with MLN8237 in multiple PDAC cell lines. This is in contrast to earlier studies using predominantly overexpression studies to assess a role for AAK in RalA localization. Although, Counter and colleagues (10) did demonstrate localization changes of RalA with AAK RNAi, these studies were limited to one cell line. We found no localization changes of RalA with pharmacologic inhibition of AAK in four of four PDAC cell lines examined. Therefore differences in AAK effects on RalA localization may be due inherent difference between genetic and pharmacologic inhibition of AAK.

Overall, response to MLN8237 was promising in the PDX model. Of the seven PDX tumors that we treated with 30 mg/kg (MTD) of MLN8237, three demonstrated TGI and one exhibited regression. These data highlight the potential effectiveness of MLN8237 treatment in a subset of patients and emphasize the importance of identifying a biomarker of response. Although we observed that MLN8237 is effective in a subset of human tumors in our PDX model, this response was not associated with basal phosphorylation levels of RalA at S194 or changes in mitotic index.

The upstream Aurora A activator TPX2 (targeting protein for *Xenopus* like-like protein 2) was recently identified as predictive biomarker for the Aurora A-specific inhibitor MK-8745 in non-Hodgkin lymphoma cells (43). Except for this example, very few predictive biomarkers have been characterized for AAK inhibitor responsiveness. Therefore, it is of great interest that Ki67 does appear to be an early biomarker of response in PDAC PDX. More studies will be needed to determine if baseline Ki67 is a predictive biomarker of response to MLN8237.

In conclusion, we have determined that Aurora A activity as determined by auto-phosphorylation and RalA S194 phosphorylation levels are elevated in a subset of PDAC cell lines and tumors. Elevated Aurora A activity correlated with high RalA S194 phosphorylation levels. We observed variable responsiveness of PDAC cell lines and PDX to MLN8237. Basal RalA S194 phosphorylation levels or changes in RalA S194 following MLN8237 treatment were not predictive of responsiveness, indicating that other protein kinases or phosphatases may regulate S194 phosphorylation in PDAC cells. These data suggest that further investigation of MLN8237 in a subset of PDAC patients is warranted, though our preclinical data suggests that activity will be RalA-independent and that RalA S194 phosphorylation will not be a predictive biomarker of response. However, we have identified decreases in Ki67-positive cells as a potential early pharmacodynamic biomarker of response to MLN8237 in PDAC. Ki67 would be attractive as it is already widely used in clinical practice and does not suffer from the challenges of phosphospecific antibodies. Further investigation is warranted to determine the clinical feasibility of utilizing Ki67 as a pharmacodynamic biomarker. Finally, it appears that AAK-mediated phosphorylation of RalA S194 is not an effective way to target RalA signaling in PDAC and further investigation is needed to determine other potential kinases that can be targeted.

Supplementary Material

Refer to Web version on PubMed Central for supplementary material.

Acknowledgments

Financial support: This work was supported by Public Health Service grants CA042978 (C.J. Der) and CA140424 (J.J. Yeh) from the National Cancer Institute. N.F. Neel was supported by a fellowship from the American Cancer Society (18777-PF-10-023-01-CSM).

We acknowledge Charlene Santos and the UNC Animal Studies Core for all their work on the animal studies, the Translational Pathology Laboratory Core for tissue processing, and the Tissue Procurement Core facilities for tumor acquisition. We would also like to thank Richard Moffitt and Pei Fen Kuan for guidance in some of the statistical analyses.

GRANT SUPPORT

This work was supported by CA042978 (C.J. Der) and CA140424 (J.J. Yeh) from the National Cancer Institute and the American Surgical Foundation (J.J. Yeh), and the American Cancer Society (18777-PF-10-023-01-CSM; N.F. Neel).

References

1. Siegel R, Naishadham D, Jemal A. Cancer statistics, 2012. CA Cancer J Clin. 2012; 62:10–29. [PubMed: 22237781]
2. Hezel AF, Kimmelman AC, Stanger BZ, Bardeesy N, Depinho RA. Genetics and biology of pancreatic ducal adenocarcinoma. Genes Dev. 2006; 20:1218–49. [PubMed: 16702400]
3. Yeh JJ, Der CJ. Targeting signal transduction in pancreatic cancer treatment. Expert Opin Ther Targets. 2007; 11:673–94. [PubMed: 17465725]
4. Bodemann BO, White MA. Ral GTPases and cancer: linchpin support of the tumorigenic platform. Nat Rev Cancer. 2008; 8:133–40. [PubMed: 18219307]
5. Neel NF, Martin TD, Stratford JK, Zand TP, Reiner DJ, Der CJ. The RalGEF-Ral Effector Signaling Network: The Road Less Traveled for Anti-Ras Drug Discovery. Genes Cancer. 2011; 2:275–87. [PubMed: 21779498]
6. Lim KH, O'Hayer K, Adam SJ, Kendall SD, Campbell PM, Der CJ, et al. Divergent roles for RalA and RalB in malignant growth of human pancreatic carcinoma cells. Curr Biol. 2006; 16:2385–94. [PubMed: 17174914]

7. Lim KH, Baines AT, Fiordalisi JJ, Shipitsin M, Feig LA, Cox AD, et al. Activation of RalA is critical for Ras-induced tumorigenesis of human cells. Cancer Cell. 2005; 7:533–45. [PubMed: 15950903]
8. Sablina AA, Chen W, Arroyo JD, Corral L, Hector M, Bulmer SE, et al. The tumor suppressor PP2A Abeta regulates the RalA GTPase. Cell. 2007; 129:969–82. [PubMed: 17540176]
9. Wu JC, Chen TY, Yu CT, Tsai SJ, Hsu JM, Tang MJ, et al. Identification of V23RalA-Ser194 as a critical mediator for Aurora-A-induced cellular motility and transformation by small pool expression screening. J Biol Chem. 2005; 280:9013–22. [PubMed: 15637052]
10. Lim KH, Brady DC, Kashatus DF, Ancrile BB, Der CJ, Cox AD, et al. Aurora-A phosphorylates, activates, and relocalizes the small GTPase RalA. Mol Cell Biol. 2010; 30:508–23. [PubMed: 19901077]
11. Kashatus DF, Lim KH, Brady DC, Pershing NL, Cox AD, Counter CM. RALA and RALBP1 regulate mitochondrial fission at mitosis. Nat Cell Biol. 2011; 13:1108–15. [PubMed: 21822277]
12. Grandemange S, Herzig S, Martinou JC. Mitochondrial dynamics and cancer. Semin Cancer Biol. 2009; 19:50–6. [PubMed: 19138741]
13. Marumoto T, Zhang D, Saya H. Aurora-A - a guardian of poles. Nat Rev Cancer. 2005; 5:42–50. [PubMed: 15630414]
14. Goepfert TM, Adigun YE, Zhong L, Gay J, Medina D, Brinkley WR. Centrosome amplification and overexpression of aurora A are early events in rat mammary carcinogenesis. Cancer Res. 2002; 62:4115–22. [PubMed: 12124350]
15. Sakakura C, Hagiwara A, Yasuoka R, Fujita Y, Nakanishi M, Masuda K, et al. Tumour-amplified kinas BTAK is amplified and overexpressed in gastric cancers with possible involvement in aneuploid formation. Br J Cancer. 2001; 84:824–31. [PubMed: 11259099]
16. Tanaka T, Kimura M, Matsunaga K, Fukada D, Mori H, Okano Y. Centrosomal kinas AIK1 is overexpressed in invasive ducal carcinoma of the breast. Cancer Res. 1999; 59:2041–4. [PubMed: 10232583]
17. Jeng YM, Peng SY, Lin CY, Hsu HC. Overexpression and amplification of Aurora-A in hepatocellular carcinoma. Clin Cancer Res. 2004; 10:2065–71. [PubMed: 15041727]
18. Lassus H, Staff S, Leminen A, Isola J, Butzow R. Aurora-A overexpression and aneuploidy predict poor outcome in serous ovarian carcinoma. Gynecol Oncol. 2011; 120:11–7. [PubMed: 20937525]
19. Wang J, Yang S, Zhang H, Song Y, Zhang X, Qian H, et al. Aurora-A as an independent molecular prognostic marker in gastric cancer. Oncol Rep. 2011; 26:23–32. [PubMed: 21479365]
20. Yang F, Guo X, Yang G, Rosen DG, Liu J. AURKA and BRCA2 expression highly correlate with prognosis of endometrioid ovarian carcinoma. Mod Pathol. 2011; 24:836–45. [PubMed: 21441901]
21. Anand S, Penrhyn-Lowe S, Venkitaraman AR. AURORA-A amplification overrides the mitotic spindle assembly checkpoint, inducing resistance to Taxol. Cancer Cell. 2003; 3:51–62. [PubMed: 12559175]
22. Michikawa M, Wada Y, Sano M, Uchihara T, Furukawa T, Shibuya H, et al. Radiation myelopathy: significance of gadolinium-DTPA enhancement in the diagnosis. Neuroradiology. 1991; 33:286–9. [PubMed: 1881553]
23. Tentler JJ, Tan AC, Weekes CD, Jimeno A, Leong S, Pitts TM, et al. Patient-derived tumour xenografts as models for oncology drug development. Nat Rev Clin Oncol. 2012; 9:338–50. [PubMed: 22508028]
24. Erkan M, Hausmann S, Michalski CW, Fingerle AA, Dobritz M, Kleeff J, et al. The role of stroma in pancreatic cancer: diagnostic and therapeutic implications. Nat Rev Gastroenterol Hepatol. 2012; 9:454–67. [PubMed: 22710569]
25. Erkan M, Reiser-Erkan C, Michalski CW, Kong B, Esposito I, Friess H, et al. The impact of the activated stroma on pancreatic ducal adenocarcinoma biology and therapy resistance. Curr Mol Med. 2012; 12:288–303. [PubMed: 22272725]
26. Morton CL, Houghton PJ. Establishment of human tumor xenografts in immunodeficient mice. Nat Protoc. 2007; 2:247–50. [PubMed: 17406581]

27. Rubio-Viqueira B, Jimeno A, Cusatis G, Zhang X, Iacobuzio-Donahue C, Karikari C, et al. An in vivo platform for translational drug development in pancreatic cancer. Clin Cancer Res. 2006; 12:4652–61. [PubMed: 16899615]
28. Rubio-Viqueira B, Hidalgo M. Direct in vivo xenograft tumor model for predicting chemotherapeutic drug response in cancer patients. Clin Pharmacol Ther. 2009; 85:217–21. [PubMed: 19005462]
29. Sausville EA, Burger AM. Contributions of human tumor xenografts to anticancer drug development. Cancer Res. 2006; 66:3351–4. discussion 4. [PubMed: 16585151]
30. Campbell PM, Groehler AL, Lee KM, Ouellette MM, Khazak V, Der CJ. K-Ras promotes growth transformation and invasion of immortalized human pancreatic cells by Raf and phosphatidylinositol 3-kinase signaling. Cancer Res. 2007; 67:2098–106. [PubMed: 17332339]
31. Lee KM, Nguyen C, Ulrich AB, Pour PM, Ouellette MM. Immortalization with telomerase of the Nestin-positive cells of the human pancreas. Biochem Biophys Res Commun. 2003; 301:1038–44. [PubMed: 12589817]
32. Cifone MA, Fidler IJ. Correlation of patterns of anchorage-independent growth with in vivo behavior of cells from a murine fibrosarcoma. Proc Natl Acad Sci U S A. 1980; 77:1039–43. [PubMed: 6928659]
33. Hamad NM, Elconin JH, Karnoub AE, Bai W, Rich JN, Abraham RT, et al. Distinct requirements for Ras oncogenesis in human versus mouse cells. Genes Dev. 2002; 16:2045–57. [PubMed: 12183360]
34. Baines AT, Lim KH, Shields JM, Lambert JM, Counter CM, Der CJ, et al. Use of retrovirus expression of interfering RNA to determine the contribution of activated K-Ras and ras effector expression to human tumor cell growth. Methods Enzymol. 2006; 407:556–74. [PubMed: 16757353]
35. Martin TD, Samuel JC, Routh ED, Der CJ, Yeh JJ. Activation and involvement of Ral GTPases in colorectal cancer. Cancer Res. 2011; 71:206–15. [PubMed: 21199803]
36. Wang H, Owens C, Chandra N, Conaway MR, Brautigan DL, Theodorescu D. Phosphorylation of RalB is important for bladder cancer cell growth and metastasis. Cancer Res. 2010; 70:8760–9. [PubMed: 20940393]
37. Manfredi MG, Ecsedy JA, Meetze KA, Balani SK, Burenkova O, Chen W, et al. Antitumor activity of MLN8054, an orally active small-molecule inhibitor of Aurora A kinas. Proc Natl Acad Sci U S A. 2007; 104:4106–11. [PubMed: 17360485]
38. Scholzen T, Gerdes J. The Ki-67 protein: from the known and the unknown. J Cell Physiol. 2000; 182:311–22. [PubMed: 10653597]
39. Singh A, Greninger P, Rhodes D, Koopman L, Violette S, Bardeesy N, et al. A gene expression signature associated with “K-Ras addiction” reveals regulators of EMT and tumor cell survival. Cancer Cell. 2009; 15:489–500. [PubMed: 19477428]
40. Ying H, Kimmelman AC, Lyssiotis CA, Hua S, Chu GC, Fletcher-Sananikone E, et al. Oncogenic Kras maintains pancreatic tumors through regulation of anabolic glucose metabolism. Cell. 2012; 149:656–70. [PubMed: 22541435]
41. Manfredi MG, Ecsedy JA, Chakravarty A, Silverman L, Zhang M, Hoar KM, et al. Characterization of Alisertib (MLN8237), an investigational small-molecule inhibitor of aurora A kinas using novel in vivo pharmacodynamic assays. Clin Cancer Res. 2011; 17:7614–24. [PubMed: 22016509]
42. Dar AA, Goff LW, Majid S, Berlin J, El-Rifai W. Aurora kinas inhibitors--rising stars in cancer therapeutics? Mol Cancer Ther. 2010; 9:268–78. [PubMed: 20124450]
43. Chowdhury A, Chowdhury S, Tsai MY. A novel Aurora kinas A inhibitor MK-8745 predicts TPX2 as a therapeutic biomarker in non-Hodgkin lymphoma cell lines. Leuk Lymphoma. 2011; 53:462–71. [PubMed: 21879811]

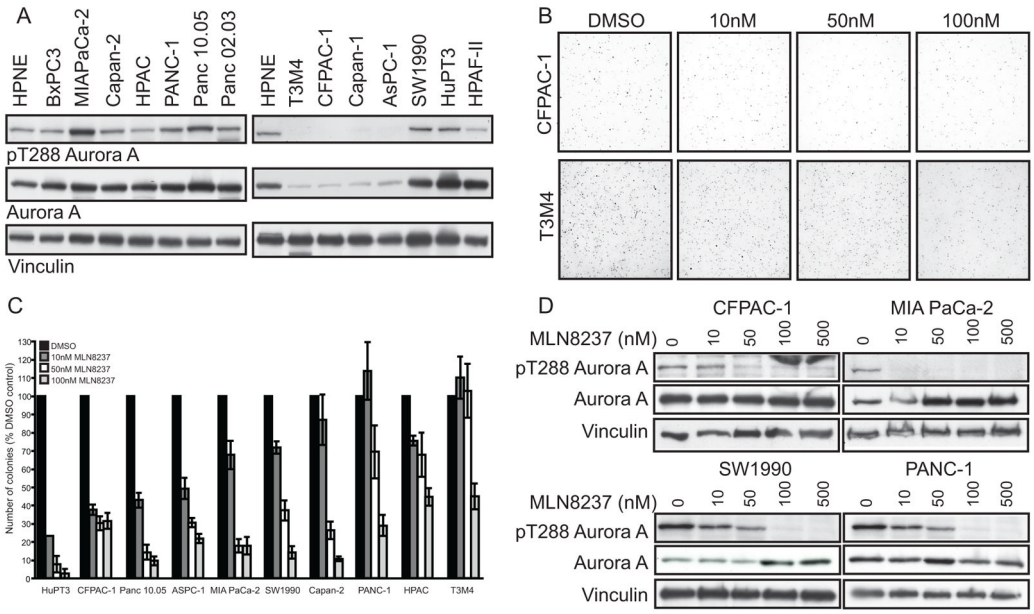

Figure 1.

Effects of MLN8237 on anchorage-dependent and -independent growth of PDAC cells are variable. A, Western blot analysis of lysates from HPNE and PDAC cell lines synchronized with a thymidine/nocodazole block using T288 Aurora A phospho-specific antibody. Total Aurora A and vinculin are shown as loading controls. B, Representative soft agar colony growth images from CFPAC-1 (IC50=4.6nM) and T3M4 cells (IC50=236.8nM). C, Anchorage-independent growth of PDAC cell lines in the presence of MLN8237. Growth is displayed in the graph as mean colony number (% DMSO control) ± SEM. D, Western blot analysis of lysates from PDAC cell lines treated with indicated doses of MLN8237 for 48 h and then synchronized with thymidine/nocodazole using the T288 Aurora A phospho-specific antibody. Total Aurora A and vinculin are shown as loading controls. Data are representative of three independent experiments.

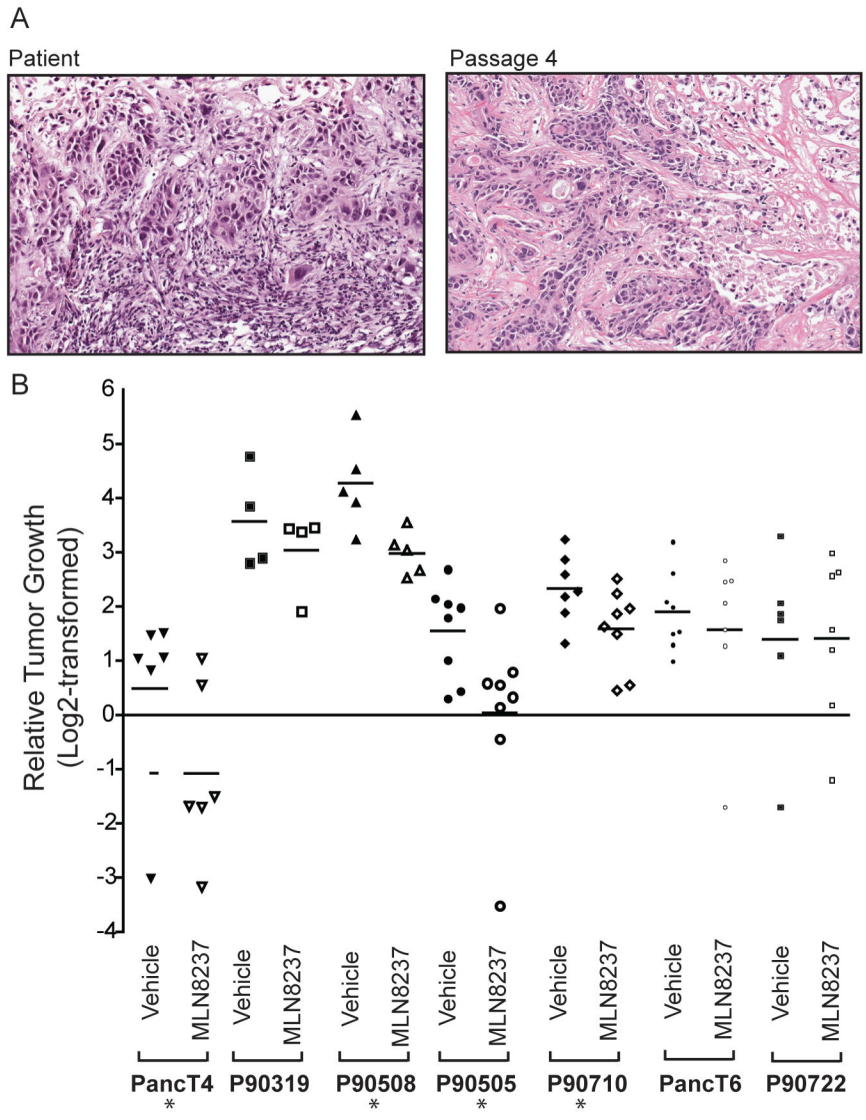

Figure 2.

MLN8237 treatment inhibits the growth of a subset of PDAC PDX. A, Hematoxylin and eosin staining of PancT6 original tumor from patient (left) and tumor from an athymic nude mouse at passage four (right). Images are shown at 100X magnification. B, Relative tumor growth of PDX at Day 28 treated with 30 mg/kg MLN8237 for 28 days. Data are displayed as Log_2-transformed relative (compared to initial tumor volume) tumor growth in at least four tumor-bearing mice per treatment. Bars represent mean. TGI-tumor growth inhibition compared to vehicle controls. * indicates significant TGI or regression (p-value ≤0.05) using Day 28 tumor volume measurements.

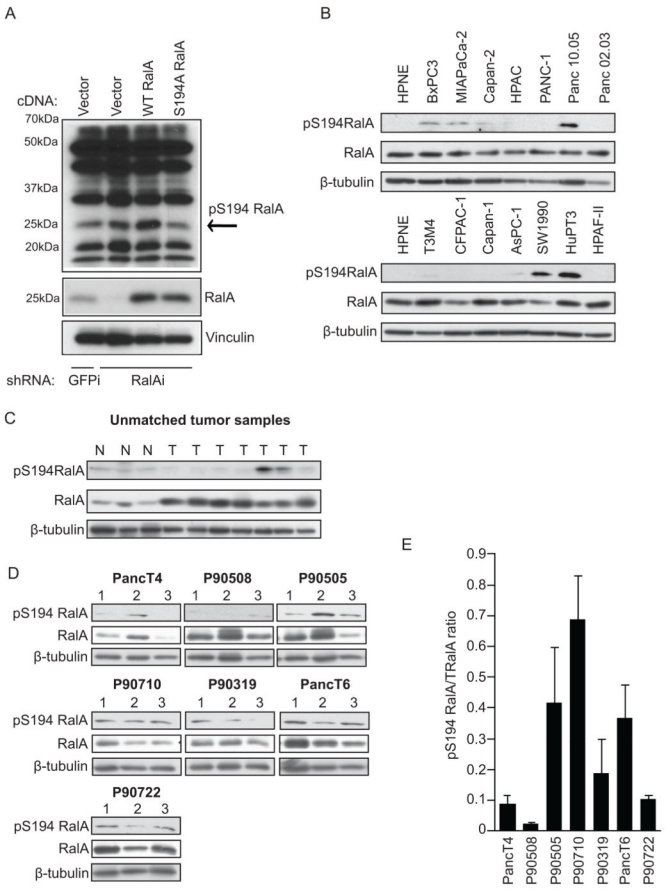

Figure 3.

RalA is phosphorylated on serine 194 in a subset of PDAC cell lines and human tumors. A, Western blot analysis of lysates from PANC-1 cells expressing GFP control or RalA-specific shRNA and RNAi-insensitive empty vector, wild type RalA, or phosphorylation-deficient (S194A) RalA using the rabbit site-specific (S194) phospho-serine RalA antibody. pS194 RalA band present at 25 kDa (indicated by the arrow) decreases in lysates expressing S194A RalA. B, Western blot analysis of lysates from HPNE and a panel of asynchronous PDAC cell lines using the S194 RalA phospho-specific antibody. Total RalA and β-tubulin are shown as loading controls. C, Western blot analysis of lysates from unmatched normal (N) and tumor (T) patient samples using the S194 RalA phospho-specific antibody. Total RalA and β-tubulin are shown as loading controls. D, Western blot analysis of PDX tumors treated with vehicle and harvested on treatment day 28 using S194 RalA phospho-specific antibody. Total RalA and β-tubulin are shown as loading controls. E, pS194 RalA to total RalA densitometry ratio quantitation of western blots in panel D. Data are representative of two or more independent experiments.

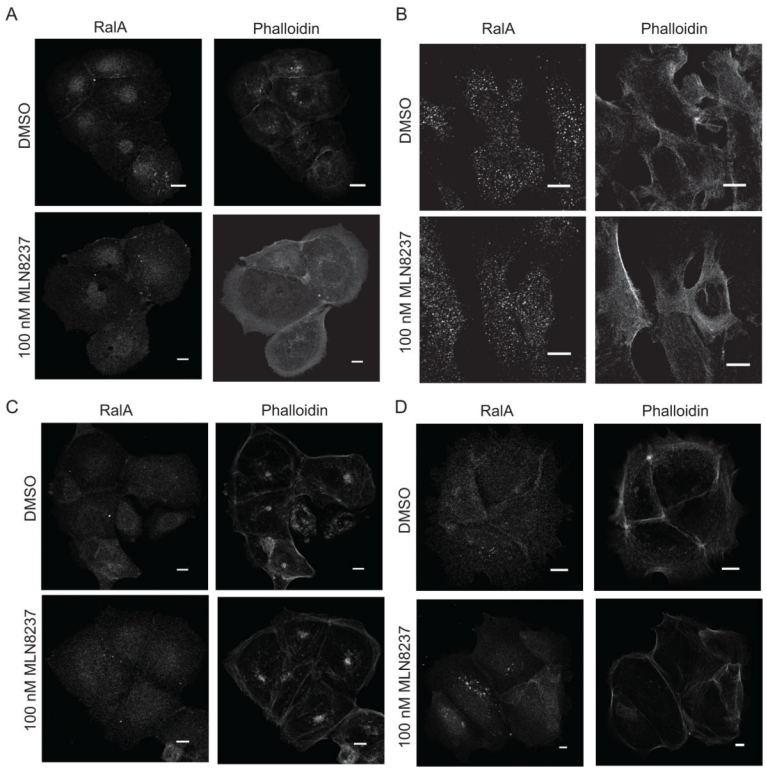

Figure 4.

MLN8237 treatment does not alter intracellular RalA localization in PDAC cell lines. A, Representative images of HuPT3 (A), CFPAC-1 (B), Panc 10.05 (C), and HPAC (D) cells immunostained with anti-RalA antibody and phalloidin following 48 h of treatment with DMSO or 100nM MLN8237. Bars, 10μm. Cells are representative of 50–100 cells visualized. Data are representative of two independent experiments.

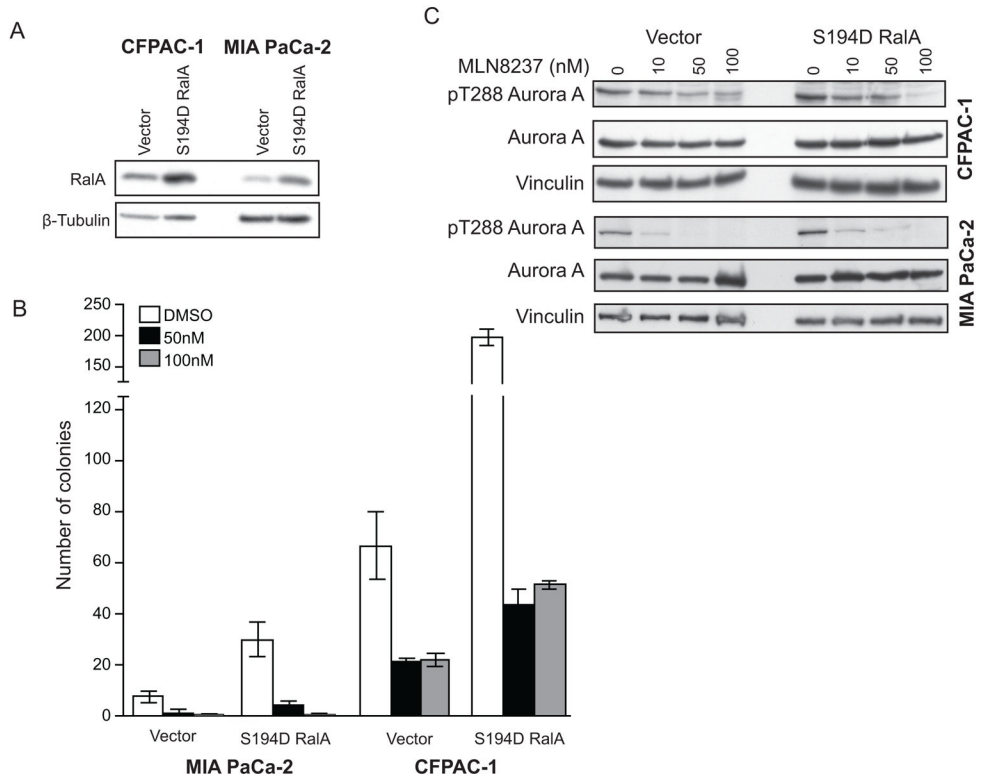

Figure 5.

Expression of phospho-mimetic (S194D) RalA does not suppress the anchorage-independent growth inhibitory effects of MLN8237. A, Western blot analysis of CFPAC-1 and MIA PaCa-2 cells expressing either empty vector or S194D RalA using a RalA-specific antibody. β-tubulin is shown as a loading control. B, Anchorage-independent growth of MIA PaCa-2 and CFPAC-1 cells expressing either empty vector or S194D RalA. Growth is displayed in the graph as mean colony number ± SEM. C, Western blot analysis of MIA PaCa-2 and CFPAC-1 cells synchronized with thymidine/nocodazole expressing either empty vector or S194D RalA and treated with indicated doses of MLN8237 for 24 h using the T288 phospho-specific Aurora A antibody. Total Aurora A and vinculin are shown as loading controls. Data are representative of at least two independent experiments.

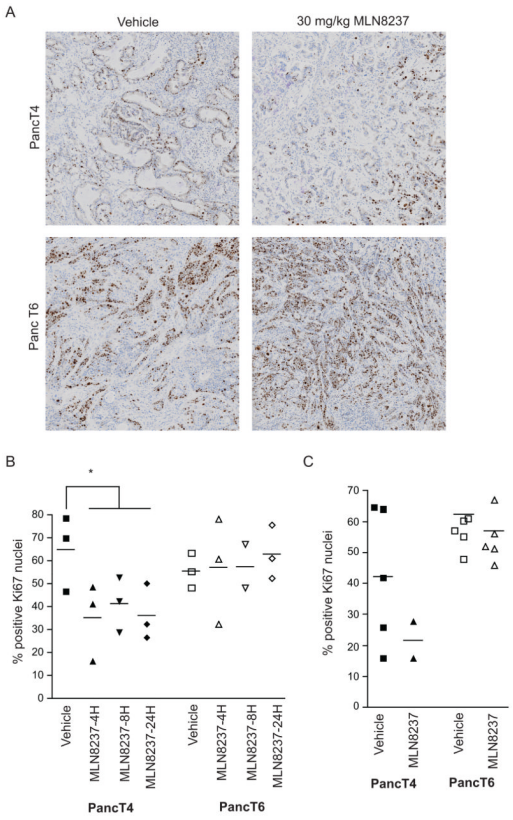

Figure 6.

Ki67 is an early biomarker for MLN8237 responsiveness. A, Representative images of Ki67 immunostaining in PancT4 and PancT6 tumors 24h after a single dose of vehicle or 30 mg/kg MLN8237. B, Percentage of Ki67-positive cells in responsive (PancT4) and non-responsive (PancT6) PDX tumors harvested at indicated times after vehicle or 30 mg/kg MLN8237 treatment. C, Percentage of Ki67-positive cells in responsive (PancT4) and non-responsive (PancT6) PDX tumors following 28 days of treatment with vehicle or 30 mg/kg MLN8237. Bars represent mean. * indicates significant differences (p-value <0.05) between vehicle treatment group and MLN8237 treatment for all time points combined.

Table 1

Calculated IC50 values based on anchorage-dependent and -independent growth for PDAC cells

	IC50 (nM)	
Cell line	**MTT**	**Soft agar**
HuPT3	830.8	3.3
CFPAC-1	9600	4.6
PANC 10.05	940.6	5
AsPC-1	Resistant*	7.6
MIA PaCa-2	1916	17.4
SW1990	Resistant*	24.1
Capan-2	2703	31
PANC-1	1890	79.7
HPAC	681.6	106
T3M4	465.4	236.8

* greater than 10,000 nM

Table 2

Summary of response of patient-derived xenograft tumors (based on tumor volume) following 28 day treatment with MLN8237 at 30 mg/kg

Tumor	Response
PancT4	Regression
P90508	63% TGI
P90505	53% TGI
P90710	39% TGI
P90319	No Response
PancT6	No Response
P90722	No Response

Table 3

Table depicting the percentage decrease in colony number in the presence of MLN8237 (50 nM and 100 nM) relative to DMSO control in MIA PaCa-2 and CFPAC-1 cells expressing either empty vector or S194D RalA

		MLN8237 (nM)	
		50nM	**100nM**
CFPAC-1	Vector	32.7 ± 1.7	33.7 ± 3.6
	S194D RalA	21.9 ± 3.3	20.1 ± 10.6
MIA PaCa-2	Vector	20.1 ± 10.6	4 ± 4
	S194D RalA	15.6 ± 5.6	2.2 ± 1.1